Title:	New perspectives for design of lightweight structures by using textile reinforced concrete
Authors:	Valeri P, Fernández Ruiz M., Muttoni A.
Published in:	fib Symposium
Pages:	8 p.
City, country:	Krakow, Poland
Year of publication:	2019
Type of publication:	Peer reviewed conference paper

Please quote as:	Valeri P, Fernández Ruiz M., Muttoni A., *New perspectives for design of lightweight structures by using textile reinforced concrete*, fib Symposium, Krakow, Poland, 2019, 8 p..

NEW PERSPECTIVES FOR DESIGN OF LIGHTWEIGHT STRUCTURES BY USING TEXTILE REINFORCED CONCRETE

Patrick Valeri[1], Miguel Fernández Ruiz[1] and Aurelio Muttoni[1]

[1] IBETON, Structural Concrete Laboratory, École polytechnique fédérale de Lausanne, Lausanne, Switzerland

Corresponding author email: miguel.fernandezruiz@epfl.ch

Abstract

Nowadays, reinforced concrete (RC) is one of the most widely spread construction materials: allowing to build robust and durable structures. Traditionally, due to cover requirements of the reinforcement and to casting and vibration needs, it has yet been associated with heavy and massive structural elements. One possible way to reduce this shortcoming has been identified as to replace steel reinforcement with non-corrosive textile fabrics. This approach known as Textile Reinforced Concrete (TRC), allows to build robust thin-walled structures.

Despite the wide spectrum of commercially available fabrics, TRC is not yet a common building solution, due to a large extent, the lack of design provisions and construction experience. In this article both topics are addressed with the aim to increase the level of knowledge on this material. First, a performance-based comparison between several fabrics is made from a material and structural point of view. Second, some construction examples of thin-walled, curved and folded precast prototypes are presented. Finally, formworking techniques and mould materials for such types of elements are discussed.

Keywords: Textile Reinforced Concrete, Tensile behaviour, Flexural response, Formworking.

1. Introduction

First modern concrete structures appeared at the end of the XIXth century. These systems result from the large availability of the raw materials for concrete and low labour wages, leading to a fast development of the new construction technology. The capacity of concrete to adopt a free form provided by a mould gave designers large freedom in shaping the material, providing tailored responses to the static and architectonical needs of the works. As a result, a series of innovative projects were made possible, such as shells, folded or thin-walled cross sections, reinforced by different layers of steel grids. In these elements, the structural performance was mainly ensured by geometry and the use of the material was significantly reduced (Gargiani & Bologna 2016).

However, during the last 50 years, the scientific concerns on durability grew as well as the requirements prescribed in codes of practice: in accordance to the exposure class, a minimum concrete cover, varying from 25 to 55 mm, is recommended in order to control rebar corrosion (EN 1992-1-1:2004). These requirements, together with the required spacing for casting, vibrating and compacting needs, yield to higher thicknesses of the reinforced concrete elements, which are currently mostly associated to robust, yet massive construction. Consequently, lightweight concrete structures, with thicknesses below 10 cm are quite rare in current reinforced concrete works.

In order to reduce restrictions on concrete cover (at least those associated to durability), non-corrosive reinforcement materials can be used replacing ordinary (metallic) bars. One of the most promising solutions is the use of high-strength textile grids (based on carbon, alkali-resistant glass or basalt fibres) that are to be used in combination with a fine-grained mortar matrix (Hegger, Zell & Horstmann 2008). The resulting material, usually named as Textile Reinforced Concrete (TRC), is a relatively new, cementitious-based, composite material that is rapidly gaining popularity as it allows casting durable structures with thicknesses below 20 mm (Scheerer 2015). This allows building with

lower amounts of material and, in addition, the clinker content can be significantly reduced, as no passivation of the reinforcement is required, enhancing consequently the sustainability character of the material.

Currently, many different textile fabrics with varying properties are available on the market, giving large freedom to designers (Scholzen et al. 2016). Most of the products come as a semi-flexible bidirectional grid, making the composite particularly attractive for the construction of double-curved structures. In addition, the number of layers and their orientation can be easily tailored with respect to the intensity and direction of the actions (Helbig et al. 2016).

2. Material behaviour

2.1. High performance cementitious mortar

For suitable casting of thin TRC elements, the concrete mix requires to have high flowability and a small aggregate size. In this paper, to explore the potential of TRC, a tailored mortar mix satisfying these requirements was used. The mortar was composed of nearly 40 % binder with low carbon blast furnace cement (CEM III/B), a low amount of high quality micro silica and nearly 60 % aggregate (quartz powder and quartz sands). The low value of the maximum aggregate size ($d_{g,max}$ = 1.60 mm) ensures the penetration of the mortar in-between the reinforcement grid even for higher reinforcement ratios. A very low water-to cement ratio was also used ($w/c \approx 0.25$) and combined with a superplasticizer to ensure high mechanical performance. The response of the mortar in compression was characterized on cylinders: $D = 70 \times H = 120$ mm. At 28 days, an average compressive strength (f_{cm}) of 110 MPa and a modulus of elasticity (E_{cm}) of 31.0 GPa were measured.

2.2. Textile Reinforcement

The textile reinforcement is composed of yarns (or filaments) grouped into rovings (bundles of yarns/strands) arranged in two directions to create a grid or fabric, see Fig. 1.

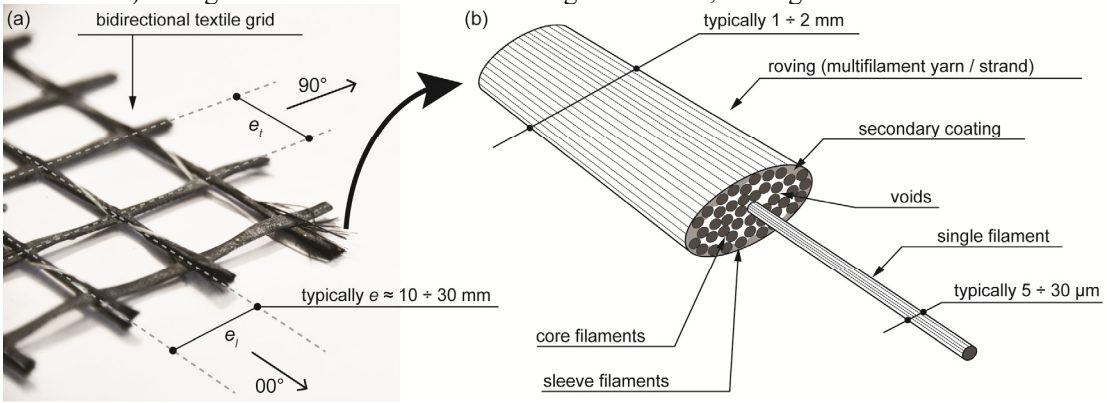

Figure 1. Fabric reinforcement: a) textile structure, b) structure of the multifilament yarn.

Yarns are made of pure raw material (carbon, glass, basalt etc..) and have a very small diameter ($\varnothing_{fil} \approx 5 - 30$ µm), presenting consequently high tensile strengths (for instance $f_{fil} \approx 5'000$ MPa for carbon fibres). Normally, a first primary coating is applied on the yarns (single filaments) in order to enhance their mechanical and durability properties.

With respect to the rovings, they are groups of hundreds or thousands of filaments, bundled together. Due to the large number of binding techniques of the yarns, it exists a wide spectrum of rovings with varying properties (Offermann et al. 2004). In addition, a secondary coating can also be applied at the surface of the roving or full impregnation of the filaments in order to enhance its properties (e.g., tensile strength, bond, etc…). The fineness of the rovings is typically measured in tex (1 tex = 1 g/km), which allows to calculate the net-cross sections of single rovings. As shown in Fig. 1, the cross-section of a roving is not completely filled by filaments and consequently the net cross-section is in general lower than the geometrical one.

Rovings are eventually woven together to form the textile fabric, that is mostly bidirectional. The mechanical performance of textile reinforcement is thus usually characterized by its tensile strength in the two principal directions (longitudinal: dir.00° and transversal: dir.90°), provided per unit width of the fabric. Due to the fact that the tensile response is usually measured on single rovings, the fabric tensile strength is calculated by dividing the unitary roving resistance by the grid spacing (Fig. 2).

Within this research project, seven fabrics were investigated in detail in terms of their mechanical properties. Their responses are presented in Fig. 2, where it can be observed that carbon fibre fabrics (CF) have in general higher strength and stiffness than glass fibre fabrics (GF).

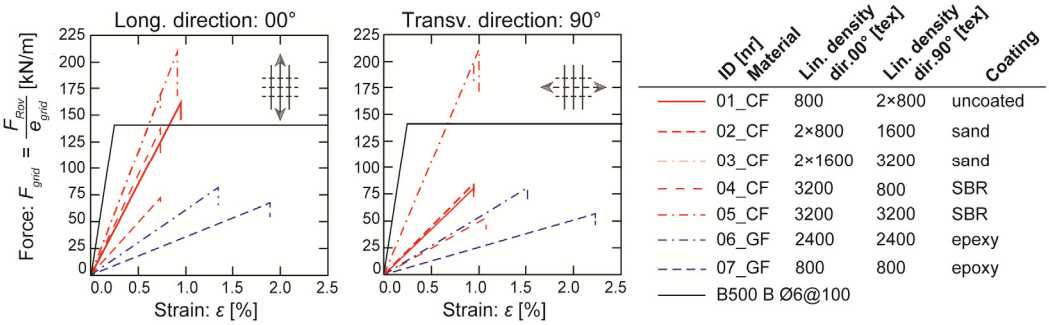

Figure 2. Selected textiles: tensile response in longitudinal (00°) and transversal (90°) directions.

Due to superior mechanical and durability character of carbon with respect to AR-glass, the two textile fabrics 01_CF and 02_CF were selected for more detailed investigation and comparison, allowing to highlight the influence of an external sand coating on the bond properties by means of tension tests on TRC ties. Their mechanical properties are summarized in table 1.

Table 1. Experimentally measured mechanical properties of the selected fabrics (average values).

Material:	01_CF		02_CF	
Direction:	dir 00	dir 90°	dir 00	dir 90°
Linear density of strand: λ_{Rov} [tex]	2 × 800	800	2 × 800	1600
Net roving cross-section: a_{Rov} [mm^2]	0.85	0.4255	0.85	0.85
Roving resistence: $F_{u,Rov}$ [N]	1600	800	1450	1700
Roving strength: f_{Rov} [MPa]	1880	1880	1700	2000
Roving modulus of elasticity: E_{Rov} [GPa]	200	200	230	210
Grid spacing: e_{grid} [mm]	10	10	20	20
Textile resistance: $F_{u,tex} = F_{u,Rov} / e_{grid}$ [kN/m]	160	79.8	72.5	85

3. Tensile behaviour of TRC

The tensile behaviour of TRC is a complex phenomenon (Contamine et al. 2014) that has been investigated in this research by means of thin plates considered as representative tensile zones in a structural member. To achieve a realistic reinforcement ratio, test specimens have been reinforced with several layers of the carbon textile fabric, aligned to the loading direction of the specimen (Fig. 3a). Tests were carried out in a clamped set-up and using displacement control with a constant rate of 1 mm/min. Deformation, crack spacing and opening were recorded by means of photogrammetric measurements. The load-strain curves shown in Fig. 3c correspond to the typical response of TRC-composites,

- Stage I: Uncracked response, when the stresses in the mortar are below its tensile strength;
- Stage II: Crack development stage, characterized by an increasing number of cracks developing for increasing load (or deformation);
- Stage III: Stabilized cracking stage, characterized by a constant number of cracks in the element, whose widths increase for increasing load (or deformation).

Failure (Fig. 3b), occurs within the Stage III in a sudden and brittle manner (without plateau), and is mainly governed by the response of the reinforcement textile. The tests show that both composites

present a good performance at load levels expected under serviceability conditions, with crack-openings not exceeding 0.2 mm even at failure. As for the crack pattern, a major role is played by the transverse reinforcement, as this acts as crack initiator. Consequently, cracks develop at a multiple n of the grid spacing (e_{grid}): $n = 3$ for the uncoated fabric ($s_{rm} = 30$ mm) and and $n = 1$ for the coated reinforcement ($s_{rm} = 20$ mm).

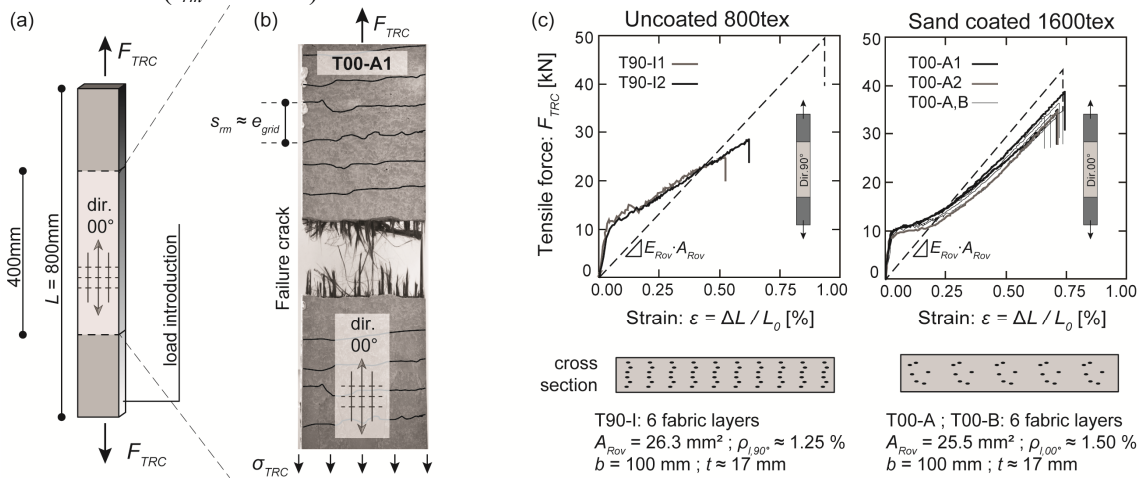

Figure 3. Tensile response of textile reinforced concrete: a) specimen, b) crack pattern and failure, c) force-strain curves and cross-section layout.

As previously described in (Valeri, Fernandez Ruiz & Muttoni 2018), the tensile response can be described by integrating the bond-slip curve in-between two adjacent cracks. Typically, the bond response between rovings and mortar results in a tri-linear response. However, also a rigid-plastic bond relationship can be assumed as a first approximation of the behaviour. The constant interface bond stress can be calculated based on the equilibrium between matrix and reinforcement between two cracks and the tension stiffening can be calculated in the stabilized cracking stage as:

$$\Delta\varepsilon_{TS} = \frac{1}{4} \cdot \frac{\tau_b \cdot U_{Rov} \cdot s_{rm}}{\eta_A \cdot a_{Rov} \cdot E_{Rov}} \tag{1}$$

Where τ_b is the bond stress, U_{Rov} the perimeter of a single roving, s_{rm} the average crack spacing and η_A an efficiency factor accounting for the non-uniform stresses of single filaments within a roving. Following the same mechanical approach, the average crack opening can be calculated as follows in the stabilized cracking stage:

$$w = s_{rm} \cdot (\varepsilon_{Rov} - \Delta\varepsilon_{TS}) = s_{rm} \left(\frac{F}{\eta_A \cdot a_{Rov} \cdot n_{Rov} \cdot E_{Rov}} - \Delta\varepsilon_{TS} \right) \tag{2}$$

Where n_{Rov} is the number of rovings in the cross-section of the specimen. With respect to the cracking (N_r) and failure (N_R) loads, they can be calculated as follows:

$$N_r = f_{ct} \cdot \left(A_{c,net} + \frac{E_{Rov}}{E_c} \cdot \eta_A \cdot a_{Rov} \cdot n_{Rov} \right) \approx f_{ct} \cdot A_c \tag{3}$$

$$N_R = \eta_A \cdot \eta_f \cdot a_{Rov} \cdot n_{Rov} \cdot f_{Rov} = EF \cdot n_{Rov} \cdot a_{Rov} \cdot f_{Rov} \tag{4}$$

Where η_f is the efficiency factor of the embedded fabric reinforcement (damage of crack lips on the filaments of a roving). Parameter EF refers to a global efficiency factor for the strength $EF = \eta_A \cdot \eta_f$.

The calculated force-strain and force-crack opening relations are plotted in Fig. 4. The results show good agreement with the experimental measurements. It can be further noted that although the bond conditions of the uncoated fabric are poorer with respect to the sand coated rovings (estimated as $\tau_b = 1.5$ MPa and $\tau_b = 2.6$ MPa respectively), tension-stiffening effects are more significant. This effect can be justified by the low activation of uncoated reinforcement ($\eta_A = 0.60$ and $\eta_A = 0.80$ respectively) as well as to the geometry of the roving, presenting a relatively larger contact surface (see table 1).

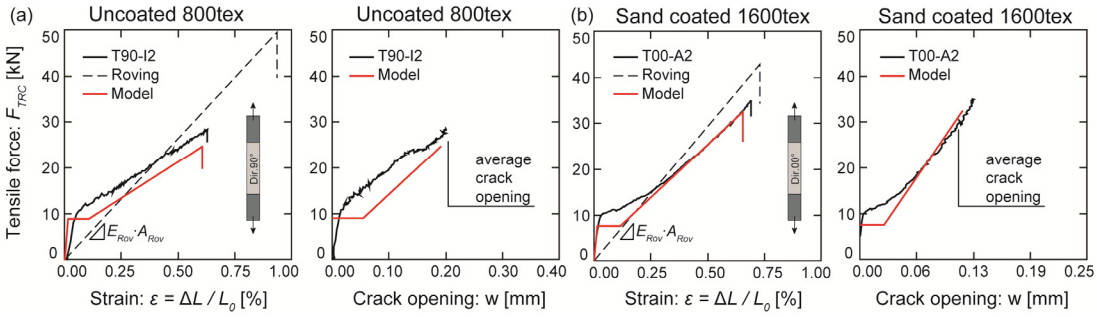

Figure 4. Calculated and experimental response: a) force-strain and force-crack opening of uncoated fabrics, specimen T90-I2, b) force-strain and force-crack opening of sand-coated fabrics, specimen T00-A2.

As for the efficiency factors of the textiles, the uncoated fabric is characterized by a higher filament efficiency ($\eta_f \approx 1.00$) but a lower global efficiency ($EF = 0.54$), whereas the coated rovings have a lower filament efficiency ($\eta_f \approx 0.95$) but a higher global efficiency ($EF = 0.76$), since more filaments can be activated.

4. Flexural behaviour of TRC

The structural response in bending was investigated on TRC linear members. To that aim, an experimental programme consisting of two full-scale elements (one double-T beam and one thin plate) was carried-out, so to compare different types of members. As shown in Fig. 5a, the plate (PV1) with a total width b of 45 cm and a thickness t of 45 mm, was reinforced with seven equally spaced double layers of uncoated carbon fabric reinforcement (dir.00). This element was tested in a four-point bending configuration generating a constant bending moment in the zone between the two forces (Fig. 6a). Differently, the double-T beam with a height of h of 290 mm and wall-thicknesses t between 15 and 20 mm (Fig. 5b) was reinforced with several layers of sand-coated carbon fabric. This member was tested in a three-point bending configuration so to avoid shear failures (Fig. 6b).

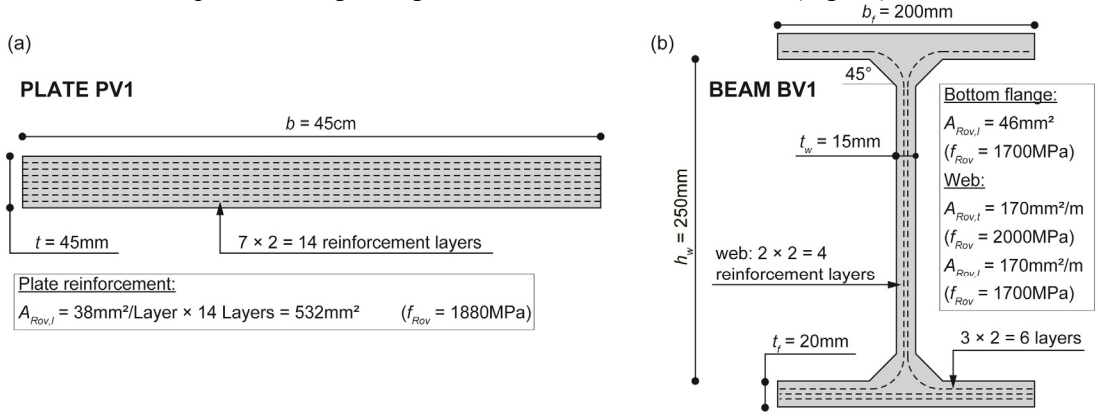

Figure 5. Cross section and reinforcement layout of the tested members: a) plate element, b) beam.

As for instrumentation, in addition to several LVDT's at mid-span, Digital Image Correlation (DIC) was used to record the crack pattern and openings. Both tests have been carried out in displacement control and neoprene pads have been placed between the specimens and the supports (and hydraulic jack) to avoid stress-concentrations.

The flexural response (in terms of moment curvature) is shown in Fig. 7. Both elements are characterized by a tri-linear response associated to the cracking of the tensile zone of the member. The average crack spacing is similar to the one recorded on specimens subjected to pure tension. Sudden failure characterized both elements, concrete crushing for the thin plate and tensile rupture of the fabric reinforcement for the beam.

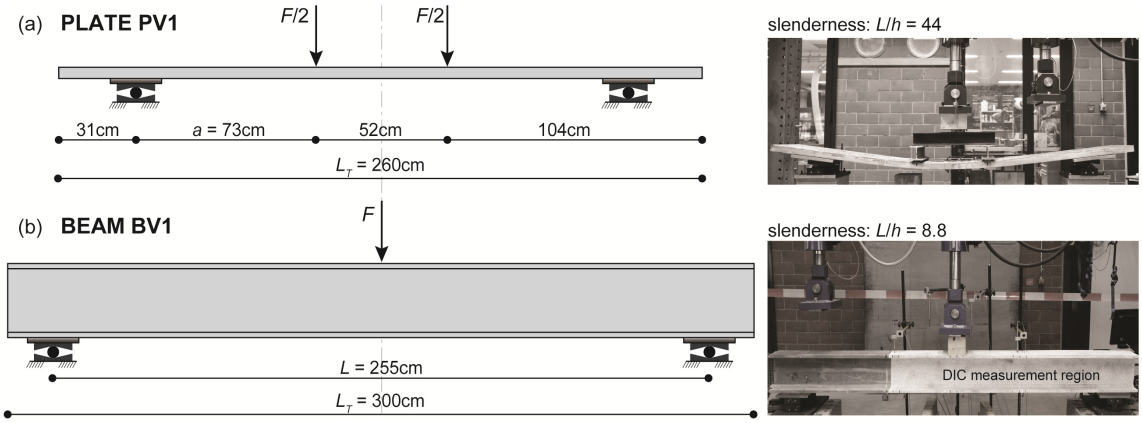

Figure 6. Specimen and test set-up for the flexural tests: a) Plate, b) beam.

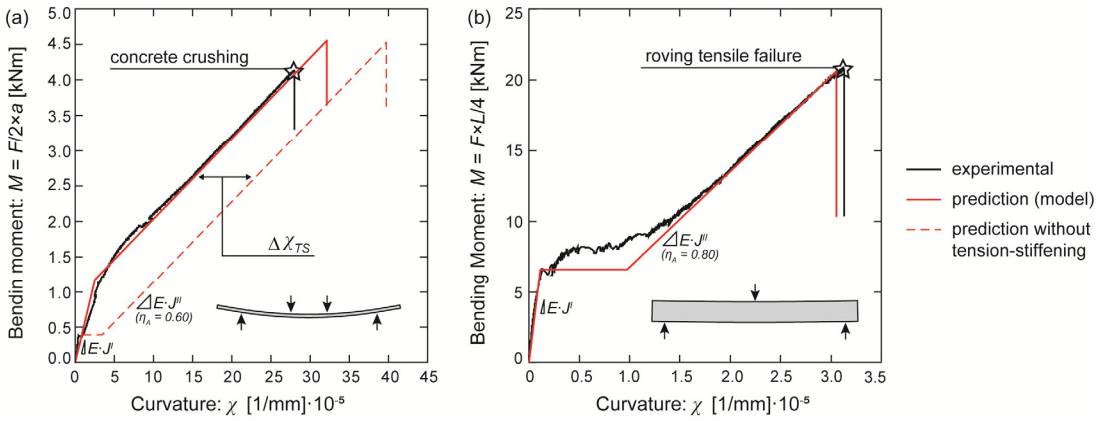

Figure 7. Experimental and calculated flexural response: a) Plate, b) double-T beam.

The bending behaviour can be modelled by means of the classic beam theory (plane sections remain plane), assuming linear-elastic material behaviour of both, high performance mortar and fabric reinforcement. The resistance is calculated assuming a linear material response up to failure (either of the mortar in compression or the rovings in tension) and neglecting the contribution of the rovings in compression. These assumpions allow to calculate the position of the neutral axis x, the curvature χ and the stresses in the components of the composite (σ_c and σ_{Rov} respectively). On that basis, the resisting bending moment M_R is calculated as:

$$M_{R,Rov} = \sum_{Rov} \left(\eta_A^i \cdot \eta_f^i \cdot \sigma_{Rov}^i \cdot a_{Rov}^i \cdot n_{Rov}^i \cdot z_{Rov}^i \right) \tag{5}$$

Where z^i_{Rov} is the inner lever arm associated to the layer i. For those reinforcement layers that are not attaining ultimate strain, the filament efficiency factor at failure is considered $\eta_f = 1.0$. For fabrics that have important tension stiffening effects (e.g. fabric 01_CF), the shift of the response can be calculated in an approximated manner (by neglecting changes in the depth of the compression zone) as:

$$\Delta X_{TS} = \frac{\Delta \varepsilon_{TS}}{d^n - x} \tag{6}$$

It is to be noted that the predicted failure load of the plate is a bit higher with respect to the experimental one, this could be justified by an irregular top surface (in terms of geometry and curing), leading to premature delamination of the concrete.

Finally, it is important to mention that although these materials behave in a more brittle manner at failure (with respect to conventional steel reinforcement), the structural deformation capacity can still be relatively high due to the strain-hardening response of the composite. Larger deformation capacities

can be achieved by more slender structures as shown by the experimental results: δ_u = 81mm and δ_u = 16mm for the tested plate and beam respectively (refer to Fig. 6 and 7).

5. Application potential

The application potential of TRC to load-bearing structures was explored within several interdisciplany projects performed in collaboration with architects (Valeri et al. 2018). One of the main aspects to consider is the formworking methods which may differ to a certain degree to those of conventional RC elements. Most of this work focused on the potential of using TRC for building light elements that can be built and erected with limited construction means, as those designed by João Filgueiras Lima in Brazil or shell structures (Valeri et al. 2018). In the following, a few examples are presented to illustrate some key aspects.

5.1. Linear elements

The X-beam shown in Fig. 8 takes inspiration from the Brazilian architect João da Gama Filgueiras Lima (Lelé) (Bo & Bardi 2000). The typical ferrocement reinforcement is replaced by carbon textile fabrics, whereas for the concentrated flexural reinforcement stainless steel rebars were used. This beam was casted using a very fluid mortar in a closed wooden formwork. A more detailed documentation of this element as well as its structural response under a three-point bending test can be found in (Valeri et al. 2018).

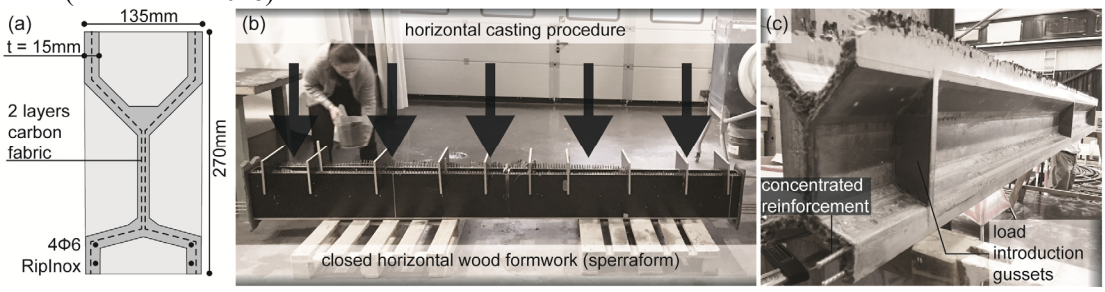

Figure 8. X-beam: a) cross-section, b) casting procedure, c) demoulded element.

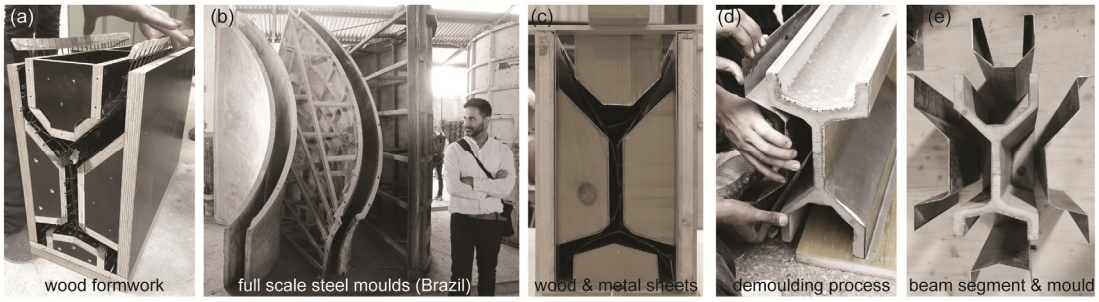

Figure 9. New formworking methods: a) classical wooden formwork, b) massive steel mould (Salvador de Bahia, Brazil), c) steel & wood mould assembly, d) demoulding, e) thin metal sheet formwork & beam segment.

Some technical visits (2017) by the authors in the Brazilian production plants in Salvador de Bahia showed that originally mostly metal formworks were used for the production line of the ferrocement elements (see Fig. 9b). Taking inspiration from the original moulds, a new hybrid technique was developed using thin metal sheets in combination with wooden stiffers. The promising method was tested on small scale elements (see Fig. 9e) and will require further investigation.

5.2. Shells

Another way to cast thin walled concrete elements, which is particularly effective for shells, are one sided moulds in combination with highly viscous mortars. The element shown in Fig. 10 has a

total length of 3 m and a thickness of $t \approx 5 - 10$ mm (of the vault) making this element weight only 96 kg.

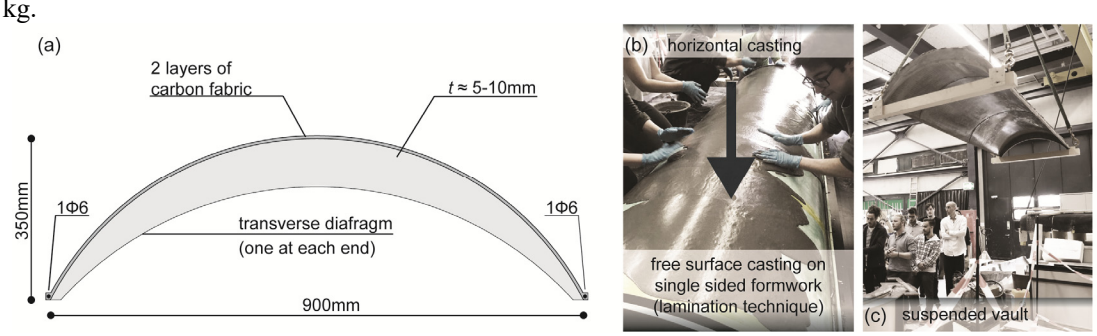

Figure 10. TRC barrel shell vault: a) cross section, b) construction, c) suspended vault.

6. Conclusions

This paper presents the results of an experimental and theoretical research focused on the material, structural behaviour, modelling approaches and application potential of Textile Reinforced Concrete. The main conclusion can be summarized as follows:

- The tensile behaviour of the composite is significantly influenced by the coating of the rovings. The latter plays a major role regarding the efficiency of the fabric reinforcement, the activation of single filaments within the strands (rigidity of tensile members / zones) and tension stiffening effects.
- With respect to structural members, it was shown that the flexural response is mainly influenced by the tensile properties of the composite. In addition, slender members may have lower resistance but present larger deformation capacities, which becomes important when designing with brittle materials.
- The application potential of TRC could be explored in thin-walled folded or curved elements that present more complex formworking with respect to traditional RC members.

Acknowledgements

The authors would like to sincerely acknowledge the support given by the association of the swiss cement producers: *cemsuisse* (research project #201407) for their financial support, providing the concrete mix and technical discussions.

References

Contamine, R., Junes, A. and Si Larbi, A. (2014) "Tensile and in-plane shear behaviour of textile reinforced concrete: Analysis of a new multiscale reinforcement," Constr. Build. Mater., vol. 51, pp. 405–413

Gargiani, R. & Bologna, A. (2016), The Rhetoric of Pier Luigi Nervi. EPFL Press.

EN 1992-1-1:2004, Eurocode 2: Design of Concrete Structures – Part 1-1: General rules and rules for buildings.

Hegger, J., Zell, M. & Horstmann, M. (2008), Textile Reinforced Concrete – Realization in applications. Tailor Made Concrete Structures – Walraven & Stoelhorst.

Scheerer, S. (2015), Was ist Textilbeton?, Beton- und Stahlbetonbau Spezial 2015 – Verstärken mit Textilbeton.

Scholzen, R. Chudoba, J. Hegger, and N. Will (2016) "Leichte Dachschalen aus Carbonbeton: Fertigteilproduktion, experimentelle Untersuchungen und Anwendungspotenzial," Beton- und Stahlbetonbau, vol. 111, no. 10, pp. 663–675.

Offermann, P., Engler, T., Gries, T. & Roye, A. (2004), Technische Textilien zur Bewehrung von Betonbauteilen, Beton- und Stahlbetonbau 99, 2004, Heft 6.

Helbig, T., Rempel, S., Unterer, K., Kulas, C. & Hegger, J. (2016), Fuß- und Radwegbrücke aus Carbonbeton in Albstadt-Ebingen, Beton- und Stahlbetonbau 111 (2016), Heft 10.

Valeri, P., Fernández-Ruiz, M. & Muttoni, A. (2018), Experimental research on textile reinforced concrete for the development of design tools, Proceedings of the 12th fib international PhD symposium in civil engineering.

Valeri, P., Guaita, P., Baur, R. & Fernández-Ruiz, M. (2018), Pedagogy through construction of thin-walled concrete elements, IV Int. conference on structural engineering without borders.

Bo, L. & Bardi, P.M. (2000), João Filgueiras Lima Lelé. Lisboa: Editorial Blau.